MEAM520

Lab: Forward Kinematics of Lynx robot

Xiaozhou Zhang

xzzhang@seas.upenn.edu

Contents

TASK 1

1 Method

1.1 Assign coordinate frames

To satisfy the constraints (DH1) and (DH2), the assignment procedure based on the DH convention could be achieved in the following steps (SHV 3.4):

Step 1: Locate and label the joint axes $z_0, \ldots, z_{n-1}$, and the position of z axes is determined by the direction of positive rotation of the joint (measured by experiment).

Step 2: Establish the base frame. Set the origin anywhere on the z_0-axis. The x_0 and y_0 axes are chosen conveniently to form a right-handed frame. In this case, the base frame is pre-chosen.

For $i = 1, \ldots, n-1$ perform Steps 3 to 5.

Step 3: Locate the origin o_i where the common normal to z_i and z_{i-1} intersects z_i. If z_i intersects z_{i-1} locate o_i at the intersection. If z_i and z_{i-1} are parallel, locate o_i in any convenient position along z_i, and in this case, these o_i are located in the intersection of z_i and link_{i-1}.

Step 4: Establish x_i along the common normal between z_{i-1} and z_i through o_i, or in the direction normal to $z_{i-1} - z_i$ plane if z_{i-1} and z_i intersect.

Step 5: Establish y_i to complete a right-handed frame.

Step 6: Establish the end-effector frame. In this case, the end-effector frame is pre-established.

The assigned of coordinate frames are shown as Figure 1-1:

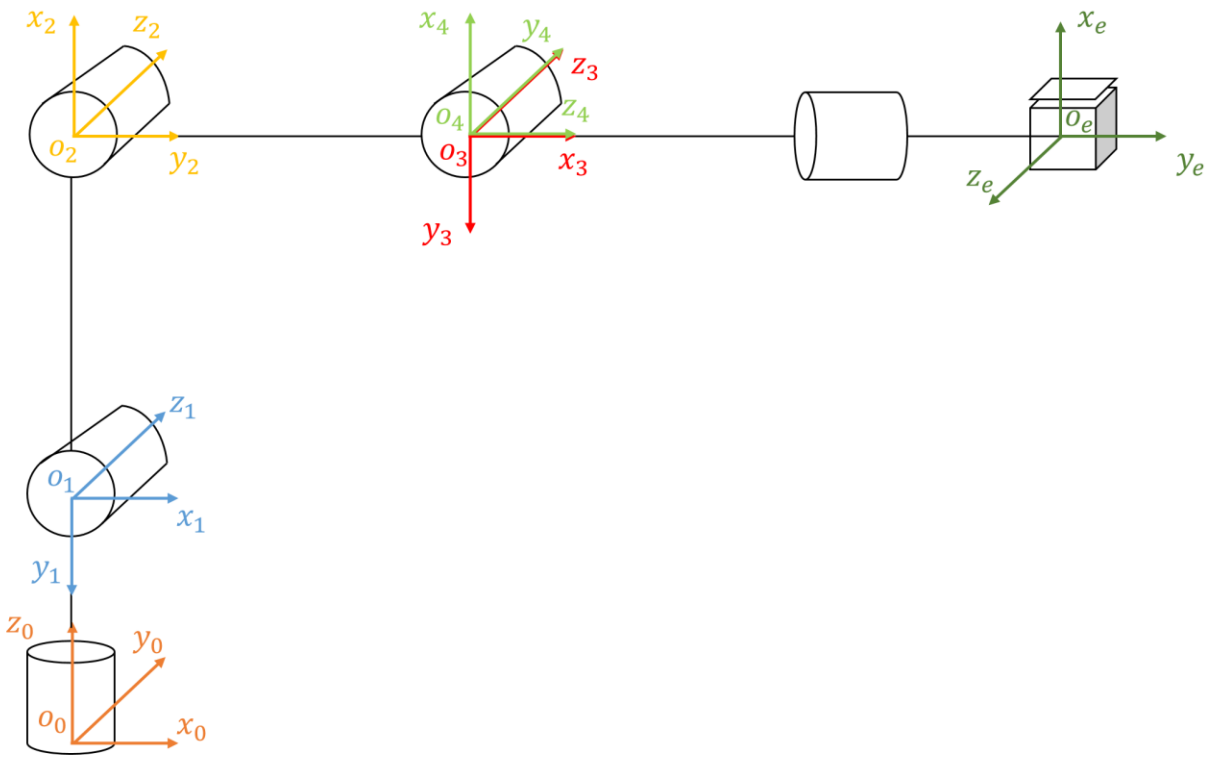

Figure 1-1 Coordinate frames assignment

1.2 Label joint angles and relevant dimensions

The directions of joint angles are observed from experiment. Since the prismatic joint does not affect end-effector's position and orientation, only the 5 revolute joint angles are labelled in Figure 1-2 along with the relevant dimensions (* variable).

Most dimensions can be obtained from the spec sheet, while the distance from joint 4 to joint 5 and the distance from joint 5 to end-effector need to be measured on the actual robot. The numerical value of these dimensions are shown in Table 1-1. The joint limits are encoded in *lynxServonPhysical.m*, shown in Table 1-2.

Dimension	l_1	l_2	l_3	l_4	l_5
Length	2.5 in	5.75 in	7.375 in	1.75 in	1.625 in

Table 1-1 Values of relevant dimensions

Joint Angle	θ_1^*	θ_2^*	θ_3^*	θ_4^*	θ_5^*
Limit (rad)	$(-1.4, 1.4)$	$(-1.2, 1.4)$	$(-1.8, 1.7)$	$(-1.9, 1.7)$	$(-2.0, 1.5)$

Table 1-2 Limits of joint angles

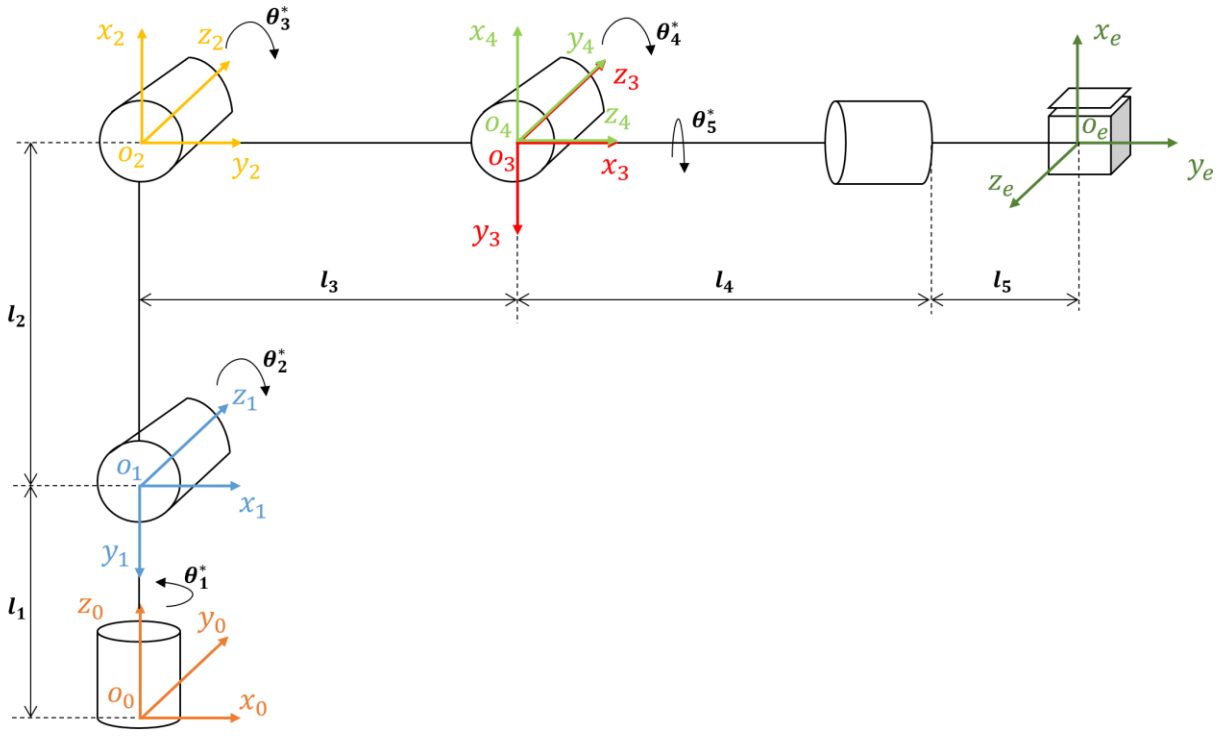

Figure 1-2 Joint angles and relevant dimensions

1.3 Determine homogenous transformation matrices

In DH convention, each homogeneous transformation A_i is represented as a product of four basic transformation, $\mathrm{Rot}_{z,\theta_i}$, Trans_{z,d_i}, Trans_{x,a_i}, and $\mathrm{Rot}_{x,\alpha_i}$. Therefore, A_i can be determined as

$$A_i = \mathrm{Rot}_{z,\theta_i}\mathrm{Trans}_{z,d_i}\mathrm{Trans}_{x,a_i}\mathrm{Rot}_{x,\alpha_i} = \begin{bmatrix} c_{\theta_i} & -s_{\theta_i}c_{\alpha_i} & s_{\theta_i}s_{\alpha_i} & a_i c_{\theta_i} \\ s_{\theta_i} & c_{\theta_i}c_{\alpha_i} & -c_{\theta_i}s_{\alpha_i} & a_i s_{\theta_i} \\ 0 & s_{\alpha_i} & c_{\alpha_i} & d_i \\ 0 & 0 & 0 & 1 \end{bmatrix} \quad (1.1)$$

where the four quantities θ_i, a_i, d_i, , α_i are parameters associated with link i and joint i (SHV 3.2).

Therefore, the homogenous transformation matrices can be obtained by following steps (SHV 3.4):

Step 1: Create a table of DH parameter a_i, d_i, α_i, θ_i.

$a_i =$ distance along x_i from the intersection of the x_i and z_{i-1} axes to o_i.

$d_i =$ distance along z_{i-1} from o_{i-1} to the intersection of the x_i and z_{i-1} axes.

$\alpha_i =$ the angle from z_{i-1} to z_i measured about x_i.

$\theta_i =$ the angle from x_{i-1} to x_i measured about z_{i-1}.

Step 2: From the homogenous transformation matrices A_i by substituting the above parameters into Equation (1.1).

The DH parameters are shown in Table 1-3.

Link	a_i	α_i	d_i	θ_i
1	0	$-\pi/2$	l_1	θ_1^*
2	l_2	0	0	$-\pi/2+\theta_2^*$
3	l_3	0	0	$\pi/2+\theta_3^*$
4	0	$-\pi/2$	0	$-\pi/2+\theta_4^*$
5	0	0	l_4+l_5	θ_5^*

Table 1-3 DH parameters for lynx robot

The A_i matrices are determined from Equation (1.1) as

$$A_1=\begin{bmatrix} c_{\theta_1^*} & 0 & -s_{\theta_1^*} & 0 \\ s_{\theta_1^*} & 0 & c_{\theta_1^*} & 0 \\ 0 & -1 & 0 & l_1 \\ 0 & 0 & 0 & 1 \end{bmatrix},$$

$$A_2=\begin{bmatrix} c_{-\pi/2+\theta_2^*} & -s_{-\pi/2+\theta_2^*} & 0 & l_2 c_{-\pi/2+\theta_2^*} \\ s_{-\pi/2+\theta_2^*} & c_{-\pi/2+\theta_2^*} & 0 & l_2 s_{-\pi/2+\theta_2^*} \\ 0 & 0 & 1 & 0 \\ 0 & 0 & 0 & 1 \end{bmatrix},$$

$$A_3=\begin{bmatrix} c_{-\pi/2+\theta_3^*} & -s_{-\pi/2+\theta_3^*} & 0 & l_3 c_{-\pi/2+\theta_3^*} \\ s_{-\pi/2+\theta_3^*} & c_{-\pi/2+\theta_3^*} & 0 & l_3 s_{-\pi/2+\theta_3^*} \\ 0 & 0 & 1 & 0 \\ 0 & 0 & 0 & 1 \end{bmatrix},$$

$$A_4=\begin{bmatrix} c_{-\pi/2+\theta_4^*} & 0 & -s_{-\pi/2+\theta_4^*} & 0 \\ s_{-\pi/2+\theta_4^*} & 0 & c_{-\pi/2+\theta_4^*} & 0 \\ 0 & -1 & 0 & 0 \\ 0 & 0 & 0 & 1 \end{bmatrix},$$

$$A_5=\begin{bmatrix} c_{\theta_5^*} & -s_{\theta_5^*} & 0 & 0 \\ s_{\theta_5^*} & c_{\theta_5^*} & 0 & 0 \\ 0 & 0 & 1 & l_4+l_5 \\ 0 & 0 & 0 & 1 \end{bmatrix}$$

1.4 Determine the position of the center of the gripper

The position and orientation of the end effector in the base frame are given by (SHV 3.1)

$$H=\begin{bmatrix} n_x & s_x & a_x & d_x \\ n_y & s_y & a_y & d_y \\ n_z & s_z & a_z & d_z \\ 0 & 0 & 0 & 1 \end{bmatrix}=\begin{bmatrix} R_e^0 & o_e^0 \\ 0 & 1 \end{bmatrix}=T_e^0=A_1A_2A_3A_4A_5 \qquad (1.2)$$

Therefore, the position of the center of the gripper $o_e^0=[d_x \quad d_y \quad d_z]^T$.

2 Evaluation

2.1 Compare the computational homogenous transformation matrices with which in the pre-lab

Using MATLAB to compute homogenous transformation matrices in the DH convention. Comparing the results with expected transformation matrices from the pre-lab, the following results are obtained:

(1) $\theta_1 = \theta_2 = \theta_3 = \theta_4 = \theta_5 = 0$

The computational homogenous transformation matrix is shown as Figure 2-1.

```
>> Evaluation
q1=?0
q2=?0
q3=?0
q4=?0
q5=?0
    0.0000    0.0000    1.0000   10.7500
   -0.0000   -1.0000    0.0000   -0.0000
    1.0000   -0.0000   -0.0000    8.2500
         0         0         0    1.0000
```

Figure 2-1 Computational homogenous transformation matrix in the first case

As a result, it matches the expected one in the pre-lab.

(2) $\theta_1 = {}^{\pi}/_{4}\ , \theta_2 = \theta_3 = \theta_4 = \theta_5 = 0$

The computational homogenous transformation matrix is shown as Figure 2-2.

```
>> Evaluation
q1=?pi/4
q2=?0
q3=?0
q4=?0
q5=?0
    0.0000    0.7071    0.7071    7.6014
   -0.0000   -0.7071    0.7071    7.6014
    1.0000   -0.0000   -0.0000    8.2500
         0         0         0    1.0000
```

Figure 2-2 Computational homogenous transformation matrix in the second case

As a result, it matches the expected one in the pre-lab.

(3) $\theta_1 = -\pi/2$, $\theta_2 = 0$, $\theta_3 = \pi/4$, $\theta_4 = 0$, $\theta_5 = \pi/2$

The computational homogenous transformation matrix is shown as Figure 2-3.

```
>> Evaluation
q1=?-pi/2
q2=?0
q3=?pi/4
q4=?0
q5=?pi/2
   -1.0000   -0.0000    0.0000    0.0000
   -0.0000    0.7071   -0.7071   -7.6014
   -0.0000   -0.7071   -0.7071    0.6486
         0         0         0    1.0000
```

Figure 2-3 Computational homogenous transformation matrix in the third case

However, the result does not match the expected one. After viewing the feedback of the pre-lab and re-observing the pose of the arm, it can be said that the expected one has been miscalculated.

The MATLAB code *evaluation.m* is listed in Appendix 1 and attached to the file.

2.2 Compute the location of all the joints and the end-effector frame expressed in the base frame

Augmenting the vector p^i, the coordinate of joint $i+1$ in the frame $o_i x_i y_i z_i$, and the vector p_i^0, the coordinate of joint $i+1$ in the base frame, by addition of a fourth component of 1 as follows,

$$P^i = \begin{bmatrix} p^i \\ 1 \end{bmatrix} \tag{2.1}$$

$$P_i^0 = \begin{bmatrix} p_i^0 \\ 1 \end{bmatrix} \tag{2.2}$$

The vector P^i is known as homogeneous representation of the vector p^i. It can be given that (SHV 2.7)

$$P_i^0 = H_i^0 P^i \tag{2.3}$$

in which

$$H_i^0 = A_1 \dots A_i$$

$$p^0 = [0 \quad 0 \quad 0]^T$$

$$p^1 = [0 \quad 0 \quad 0]^T$$

$$p^2 = [0 \quad 0 \quad 0]^T$$

$$p^3 = [0 \quad 0 \quad 0]^T$$

$$p^4 = [0 \quad 0 \quad l_4]^T$$

$$p^5 = [0 \quad 0 \quad 0]^T$$

Therefore, the location of all the joints expressed in the base frame can be obtained, shown in Table 2-1.

Joint/gripper	Location in the base frame	Equation
Joint 1	p_0^0	$P_0^0 = P^0$
Joint 2	p_1^0	$P_1^0 = A_1 P^1$
Joint 3	p_2^0	$P_2^0 = A_1 A_2 P^2$
Joint 4	p_3^0	$P_3^0 = A_1 A_2 A_3 P^3$
Joint 5	p_4^0	$P_4^0 = A_1 A_2 A_3 A_4 P^4$
Joint 6	p_5^0	$P_5^0 = A_1 A_2 A_3 A_4 A_5 P^5$

Table 2-1 Location of all the joints in base frame

The end-effector frame expressed in the base frame can be obtained from the homogeneous transformation matrix from end-effector frame to the base frame, shown as Equation (1.2).

Using MATLAB to complete previous procedures, code *calculateFK_xzzhang.m* is listed in Appendix 1 and attached to the file. A simulated zero configuration of the robot in 3D space is obtained by running predefined code *lynxStart.m*, shown as Figure 2-4.

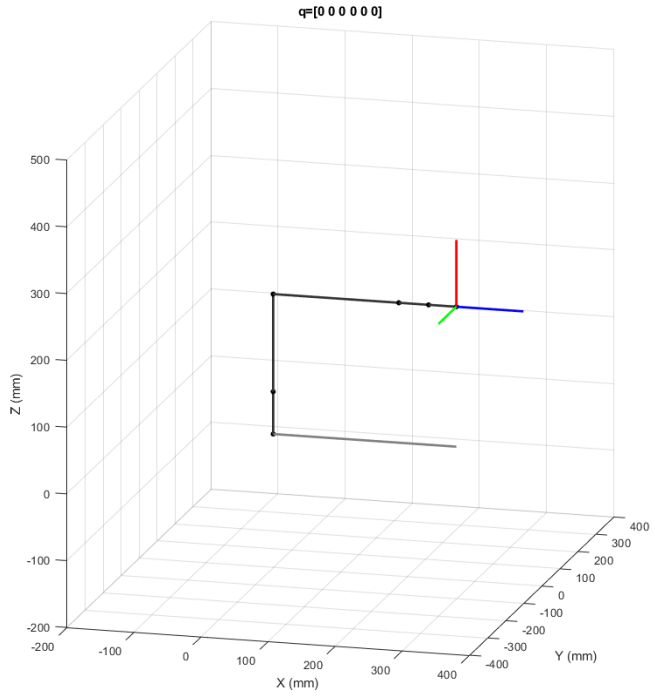

Figure 2-4 Simulated configuration of the robot in zero input

2.3 Determine the simulated configuration and physical configuration of the robot

Modifying the vector q in *lynxStart.m* and run the code, then the simulated configurations of the robot are obtained. Inputting the same vector q in *lynxServo.m*, then the physical configurations of the robot are obtained. In this lab, following 3 different inputs are chosen.

(1) $\theta_1 = {}^{\pi}/_{4}$, $\theta_2 = {}^{\pi}/_{4}, \theta_3 = \theta_4 = \theta_5 = 0$

The simulated configuration of the robot is shown in Figure 2-5 while the physical configuration of the robot is shown in Figure 2-6.

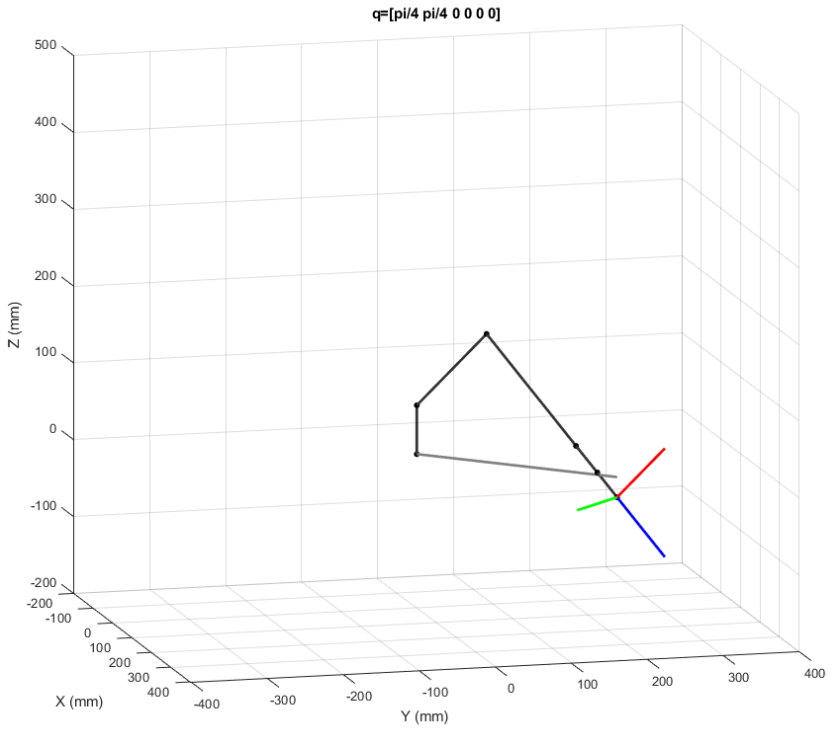

Figure 2-5 Simulated configuration of the robot on the first input

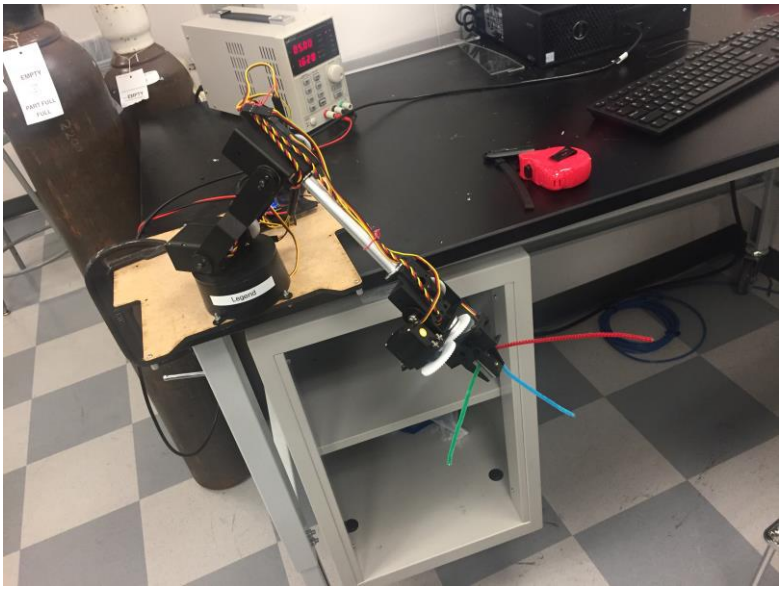

Figure 2-6 Physical configuration of the robot on the first input

(2) $\theta_1 = {}^{\pi}/_{4}$, $\theta_2 = 0$, $\theta_3 = {}^{\pi}/_{4}$, $\theta_4 = 0$, $\theta_5 = {}^{\pi}/_{2}$

The simulated configuration of the robot is shown in Figure 2-7 while the physical configuration of the robot is shown in Figure 2-8.

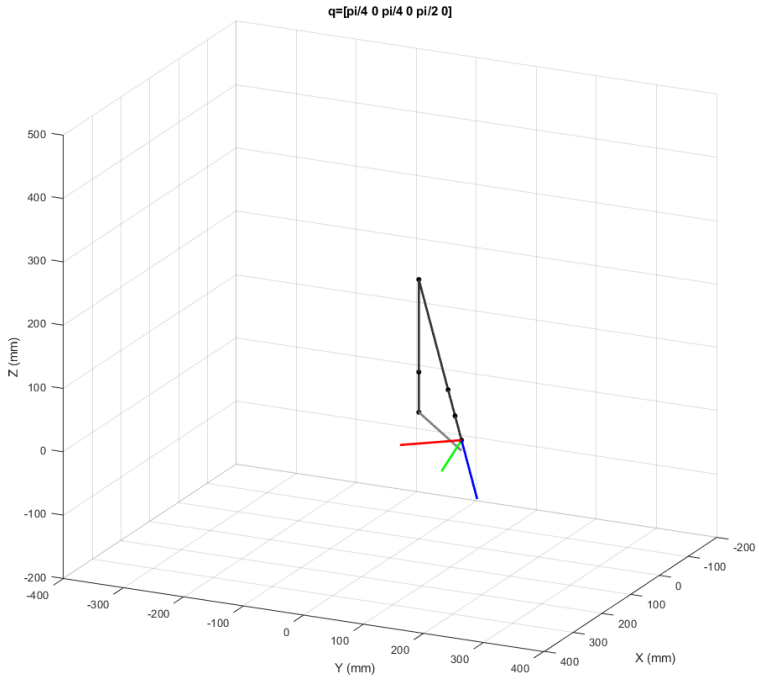

Figure 2-7 Simulated configuration of the robot on the second input

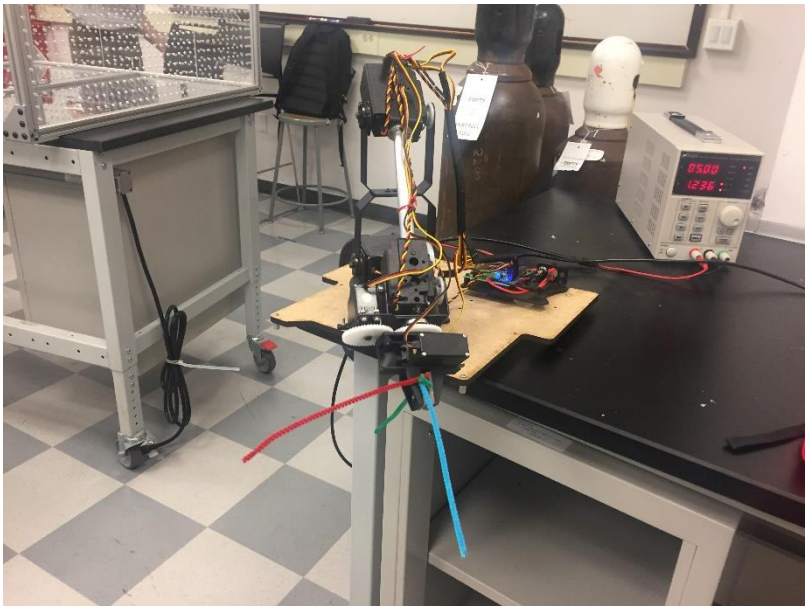

Figure 2-8 Physical configuration of the robot on the second input

(3) $\theta_1 = -\pi/2$, $\theta_2 = 0$, $\theta_3 = \pi/4$, $\theta_4 = 0$, $\theta_5 = \pi/2$

The simulated configuration of the robot is shown in Figure 2-9 while the physical configuration of the robot is shown in Figure 2-10.

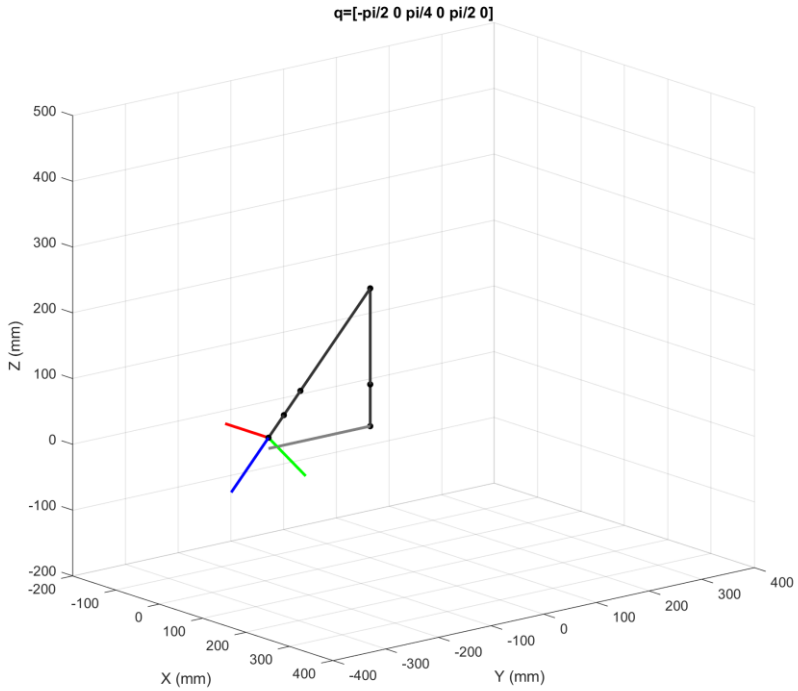

Figure 2-9 Simulated configuration of the robot on the third input

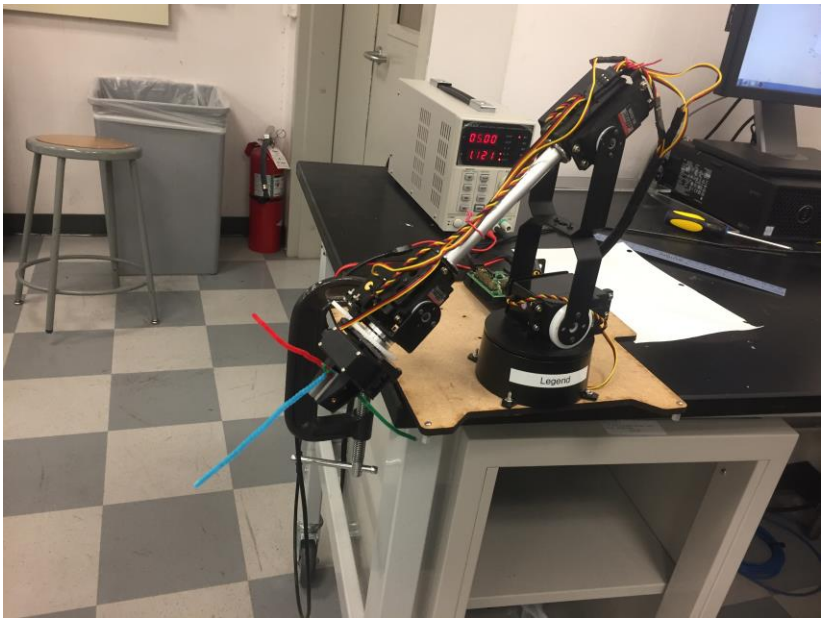

Figure 2-10 Physical configuration of the robot on the third input

3 Analysis

3.1 Differences between the simulated configurations and the physical configurations of the robot

(1) $\theta_1 = {}^{\pi}/_{4}\ ,\ \theta_2 = {}^{\pi}/_{4}, \theta_3 = \theta_4 = \theta_5 = 0$

In this case, the end-effector of the physical robot stays in its reachable workspace, so there should be no obvious differences between the simulated configuration and the physical configuration. In fact, after the measurement, there are minor differences in both the position and the orientation of the end-effector between simulation and real situation due to the precision error of the servos and the accuracy error in the dimensions' measurement.

(2) $\theta_1 = {}^{\pi}/_{4}\ , \theta_2 = 0\ , \theta_3 = {}^{\pi}/_{4}\ ,\ \theta_4 = 0\ ,\ \theta_5 = {}^{\pi}/_{2}$

In this case, the joint 5 was sent above upper limits, and was moved to 1.50 in physical input. The input differences of joint 5 does not contribute to any differences in the position of the end-effector, but it has influenced the orientation of the end-effector between simulation and real situation. The simulated orientation and physical orientation of the end-effector are shown in the rotation matrices below.

$$R^0_{e\,\text{simulated}} = \begin{bmatrix} 0.707 & -0.500 & 0.500 \\ -0.707 & -0.500 & 0.500 \\ 0 & -0.707 & -0.707 \end{bmatrix}$$

$$R^0_{e\,\text{physical}} = \begin{bmatrix} 0.741 & -0.449 & 0.500 \\ -0.670 & -0.549 & 0.500 \\ 0.050 & -0.705 & -0.707 \end{bmatrix}$$

There are also minor differences in the position of the end-effector between simulation and real situation, and minor errors in the physical orientation matrix above due to the precision error of the servos and the accuracy error in the dimensions' measurement.

(3) $\theta_1 = -{}^{\pi}/_{2}\ , \theta_2 = 0\ , \theta_3 = {}^{\pi}/_{4}\ ,\ \theta_4 = 0\ ,\ \theta_5 = {}^{\pi}/_{2}$

In this case, the joint 1 and the joint 5 were sent beyond the lower and upper limits, and were moved to -1.40 and 1.50 in physical input, respectively. The position and the orientation of the end-effector are influenced by this input differences, which are shown as followed coordinate vectors and rotation matrices below.

$$o^0_{e\,\text{simulated}} = [0\text{ in} \quad -7.601\text{ in} \quad 0.649\text{ in}]^T$$

$$o^0_{e\,\text{physical}} = [1.292\text{ in} \quad -7.491\text{ in} \quad 0.649\text{ in}]^T$$

$$R^0_{e\,\text{simulated}} = \begin{bmatrix} -1 & 0 & 0 \\ 0 & 0.707 & -0.707 \\ 0 & -0.707 & -0.707 \end{bmatrix}$$

$$R^0_{e\,\text{physical}} = \begin{bmatrix} -0.975 & -0.190 & 0.120 \\ -0.219 & 0.683 & -0.700 \\ 0.050 & -0.705 & -0.707 \end{bmatrix}$$

There are also minor errors in the position vector and the orientation matrix of the physical robot above due to the precision error of the servos and the accuracy error in the measurement.

TASK 2

4 Method

4.1 Determine the reachable workspace of the robot

The workspace of a manipulator is the total volume swept out by the end-effector as the manipulator executes all possible motions. The reachable workspace is the entire set of points reachable by the manipulators (SHV 1.1.4).

In this lab, when determining the reachable workspace of the robot is to determining all the position of the end-effector expressed in the base frame. One way to do it is to mark the position of the end-effector in a 3D plot with minor changes in each joint angles. Since the joint 5 does not affect the position of the end-effector, only the first 4 joints should be taken into account.

The strategy is to set the blow and upper limits for the first 4 joints, which are listed in the provided code *lynxServo.m.* Choose proper steps for each joint angles and using 4 loops (nested) as the inputs of the joint angles. Take the position of the end-effector expressed in the base frame as a function of 4 variables, the first 4 joints angles. Compute the positions of the end-effector expressed in the base frame on each and every inputs. Plot all the positions on a 3D map. Then the general outline of the workspace can be obtained from the map.

Using MATLAB to complete the former steps, compute the position of the end-effector, and plot a 3D map. A code *computeWorkspace_xzzhang.m* is listed in Appendix 1 and attached to the file. The reachable workspace of the robot is shown as Figure 4-1, Figure 4-2, Figure 4-3, and Figure 4-4.

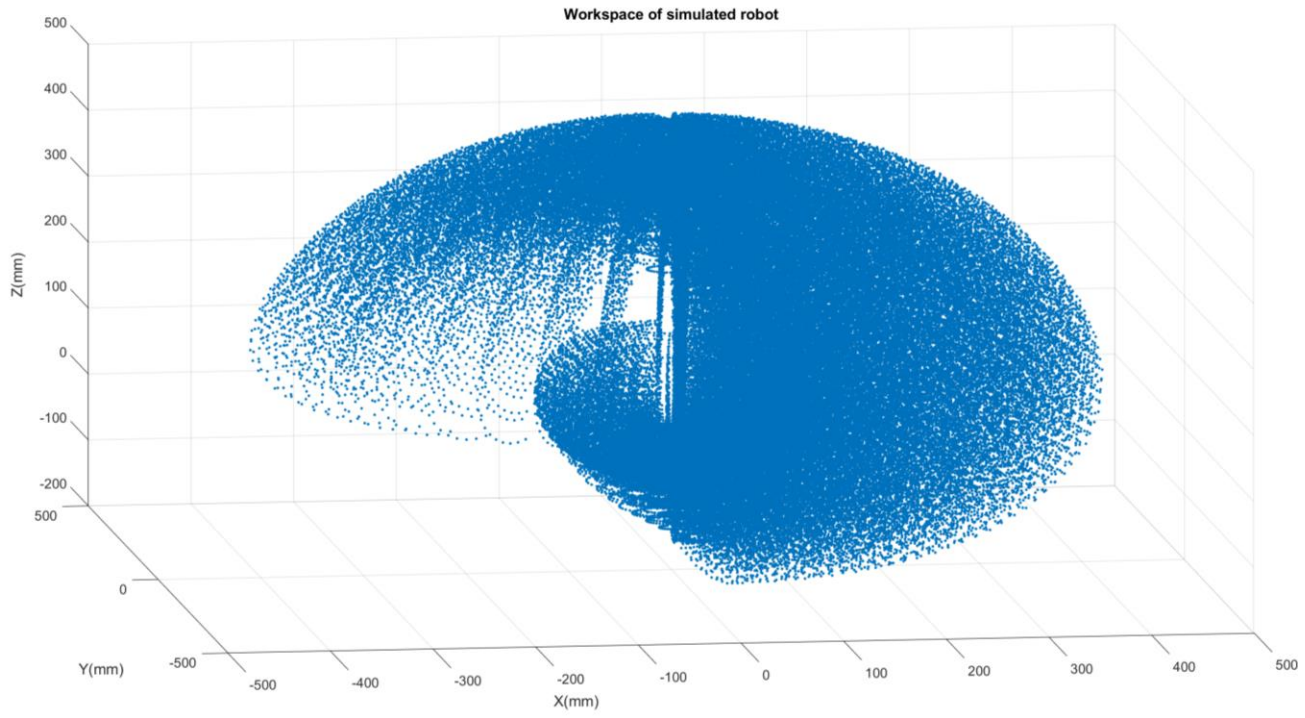

Figure 4-1 Simulated workspace of the robot

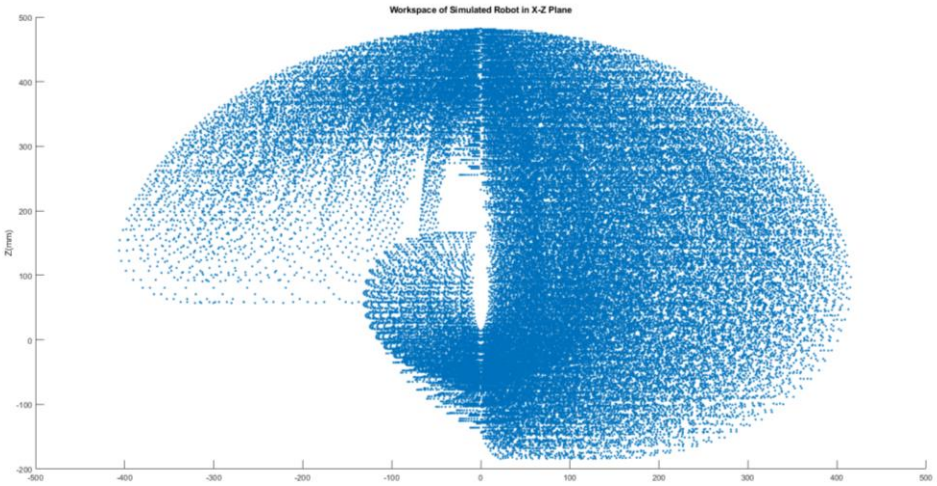

Figure 4-2 Simulated workspace of the robot projecting on X-Z plane

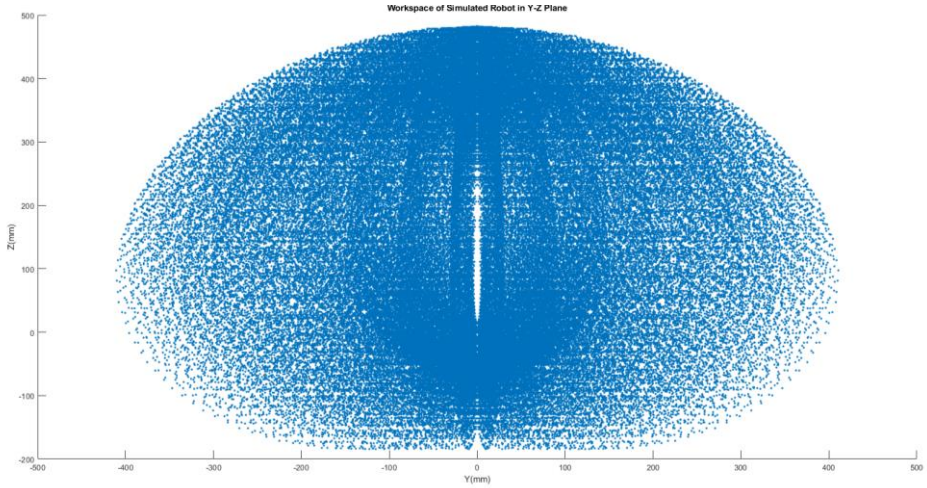

Figure 4-3 Simulated workspace of the robot projecting on Y-Z plane

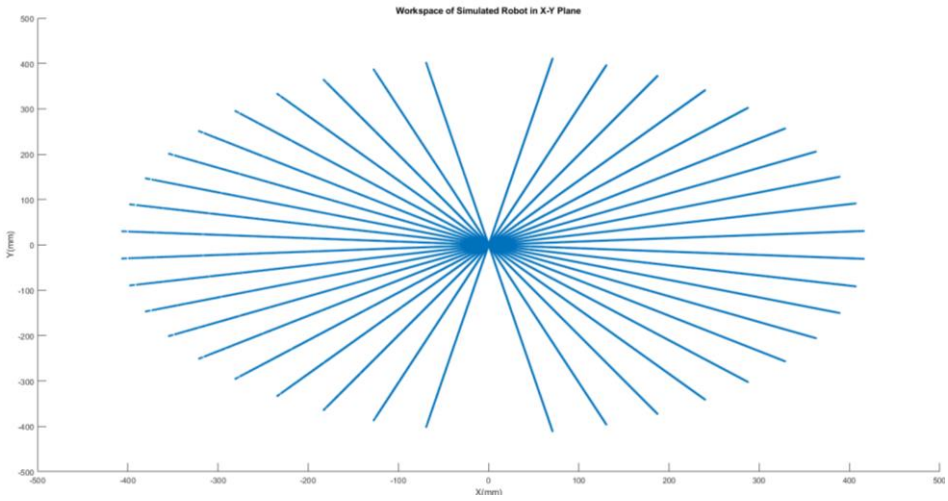

Figure 4-4 Simulated workspace of the robot projecting on X-Y plane

5 Evaluation

5.1 Compare the simulated workspace and the achievable workspace by the physical robot

The work environment of the physical robot is shown as Figure 5-1.

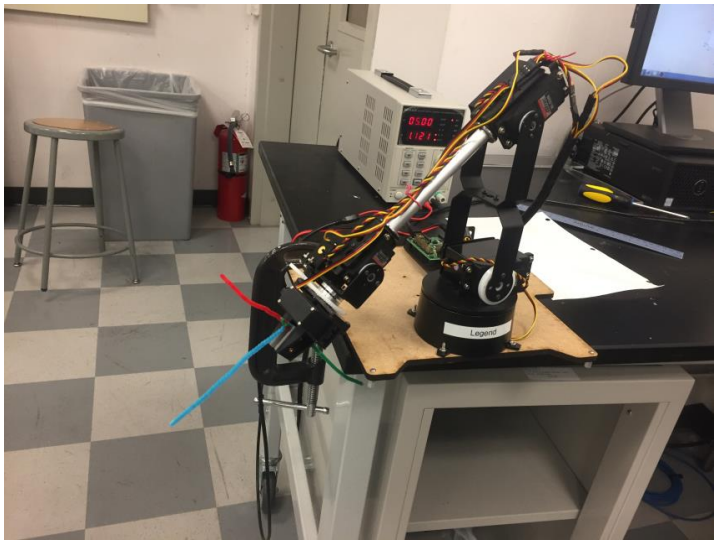

Figure 5-1 Work environment of the robot

From the figure above, one can tell that the physical workspace is constrained not only by mechanical constrains on the joint, but also by the geometry of the work environment and the geometry of the manipulator itself. So there are points that the simulation stated were valid that the robot cannot reach (i.e. some points on and below the table).

Drawing the top and two side surface of the table as 3 planes in MATLAB, there are some points which are blocked by the table, and such points are definitely not achievable by the physical robot. The drawing is shown as Figure 5-2.

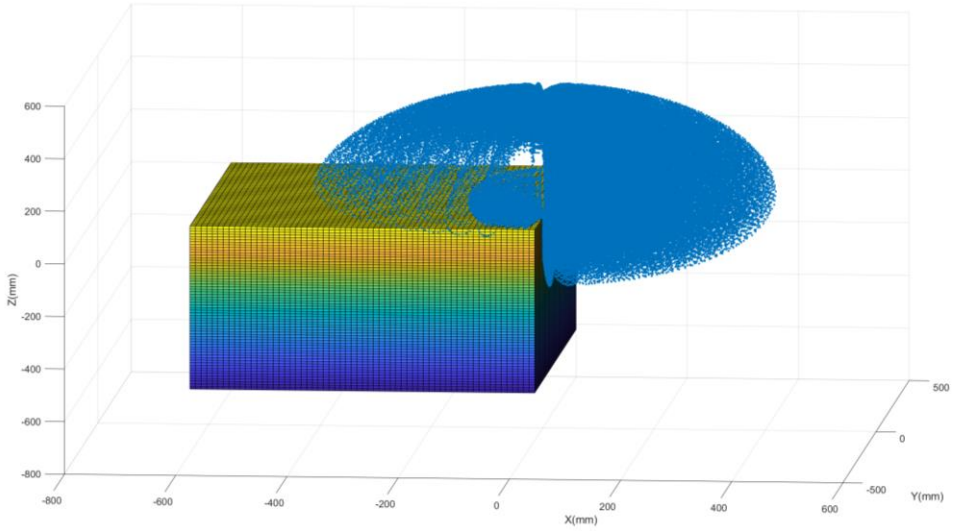

Figure 5-2 Simulated workspace with the existence of the table

Due to the precision error of the servos, there are also some points that the robot can reach that were not in simulation. For example, after measuring the actual upper limits of joint 1, it is a little bit bigger than the predefined one, 1.40 rad, approximately 1.43 rad. When angle of joint 1 exceeds 1.40 rad, there are positions that is achievable by the physical robot while not shown in simulation. A drawing of that is shown as Figure 5-3, in which in blue points are the simulated positions while the red points are the position the end-effector can reach but not shown in the simulation projecting on X-Y plane.

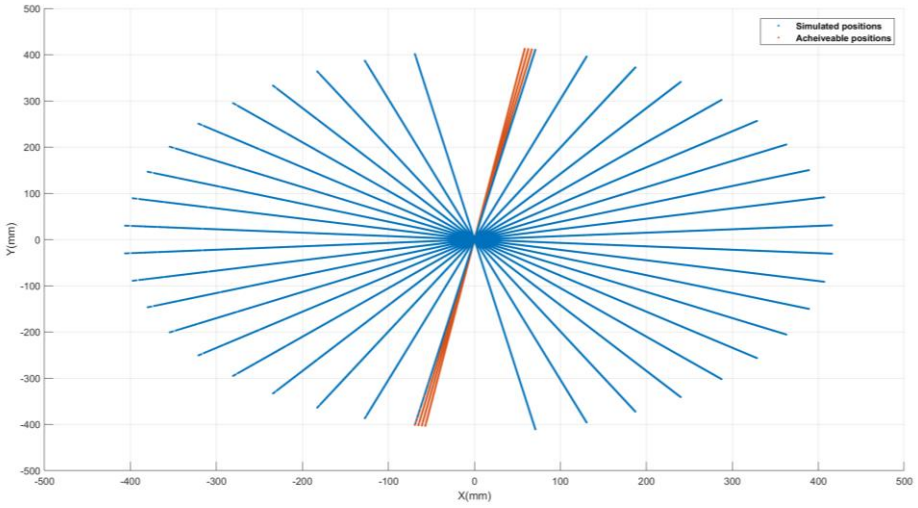

Figure 5-3 Simulated workspace vs achievable workspace projecting on X-Y plane

Similarly, due to the accuracy error in the dimensions' measurement, there can be some points that the robot can reach while is not shown in simulation. For example, if the real dimension of link 2 is 5.8 in rather than what is listed in DH convention, 5.75 in, there are positions that is achievable by the physical robot while not shown in simulation. A drawing of that is shown as Figure 5-4, in which in blue points are the simulated positions while the red points are the position the end-effector can reach but not shown in the simulation projecting on X-Y plane.

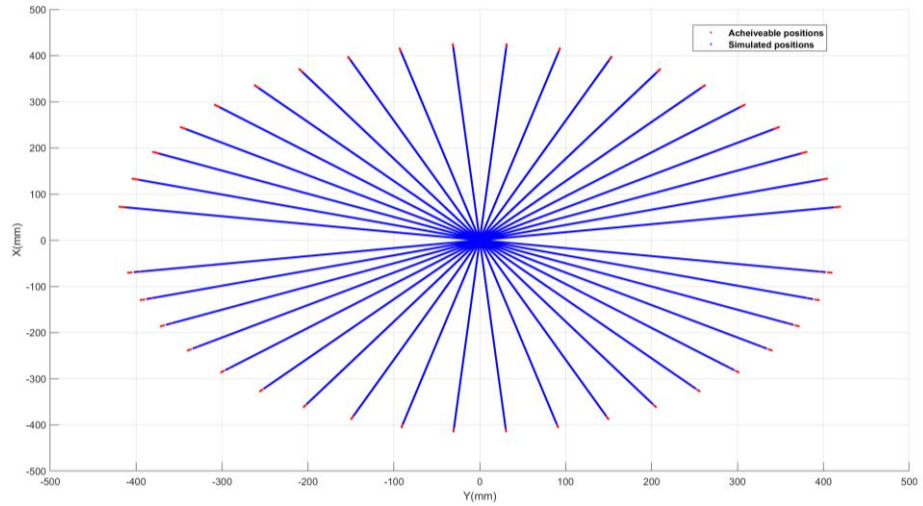

Figure 5-4 Simulated workspace vs achievable workspace projecting on X-Y plane

6 Analysis

6.1 Differences between the workspace of simulated and physical robot

As what is formerly stated, both the workspace has the positions which the other one does not contain. However, the precision error of the servos and the accuracy error in the dimensions' measurement are minor that they might be ignored in this analysis. Then the only differences between the workspace of simulated and physical robot are the positions that cannot be achieved by the physical robot but are shown in the simulations.

Positions that are not achievable in the physical situation are due to the geometry constrains in the robot and work environment. the After experiments, all the constrains can be concluded as the following three categories.

(1) Conflict with in the robot arms

Link 2 has a support plate around the middle of it. That can cause conflicts with link 3.

This type of conflict is shown as Figure 6-1 and there is a video (Video 1) showing the procedure of the conflict listed in Appendix 2.

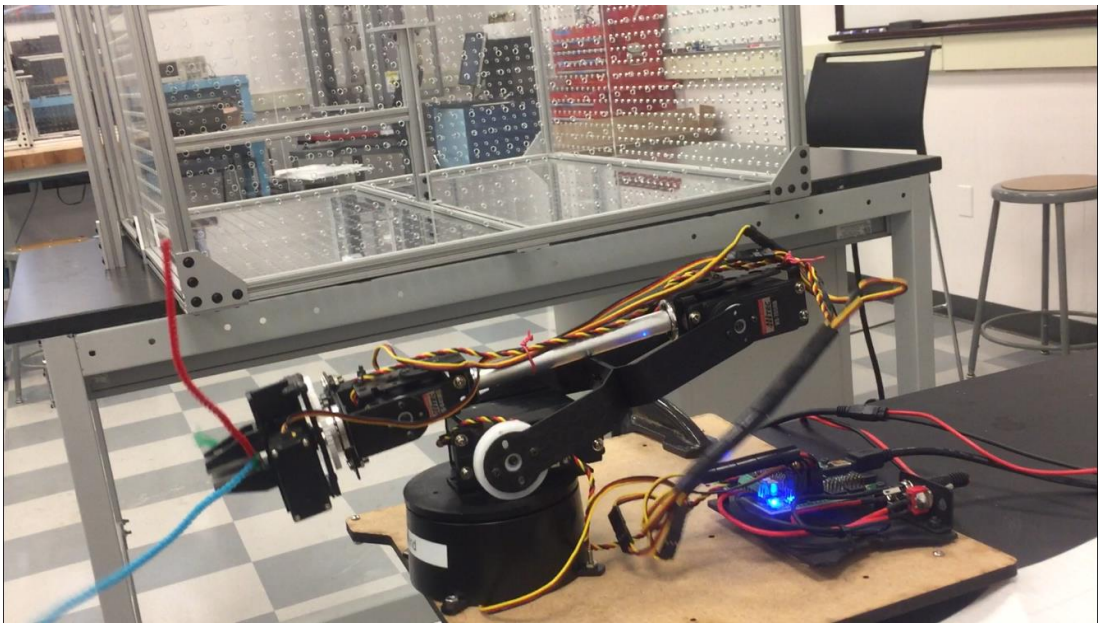

Figure 6-1 Conflict between link 2 and link 3

(2) Conflict between the robot and the environment

As what is stated in 5.1, there must be conflict between the robot arms and the table. The conflict part of the robot are end-effector, link 5, link 4, and link 3. The conflict part of the can be the top, the front, and the left side of the table.

This type of conflict is shown as Figure 6-2 and Figure 6-3. There are two videos (Video 2 and Video 3) showing the procedure of the conflict listed in Appendix 2.

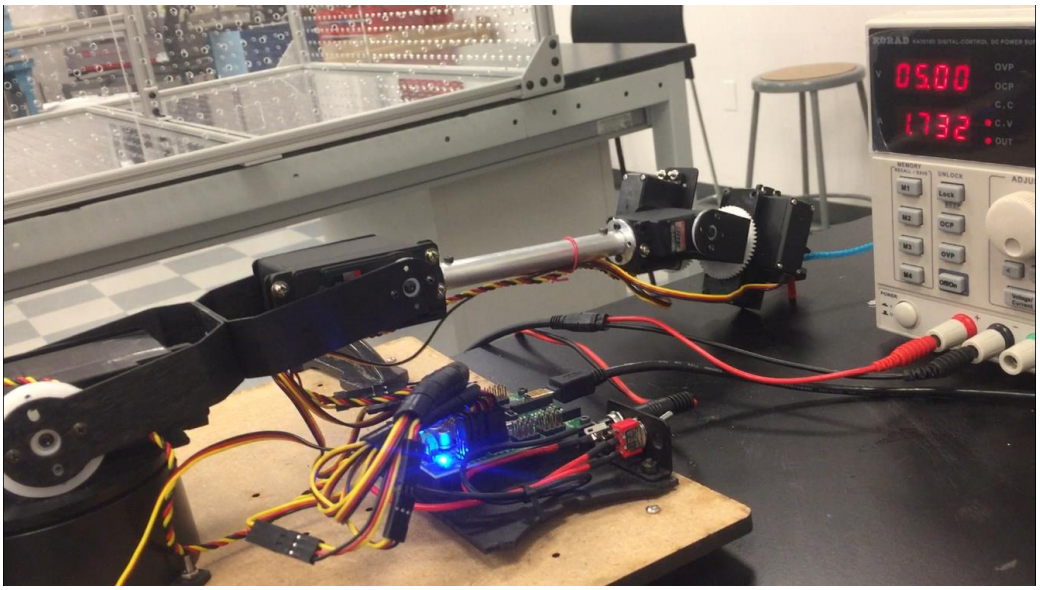

Figure 6-2 Conflict between end-effector and the top side of the table

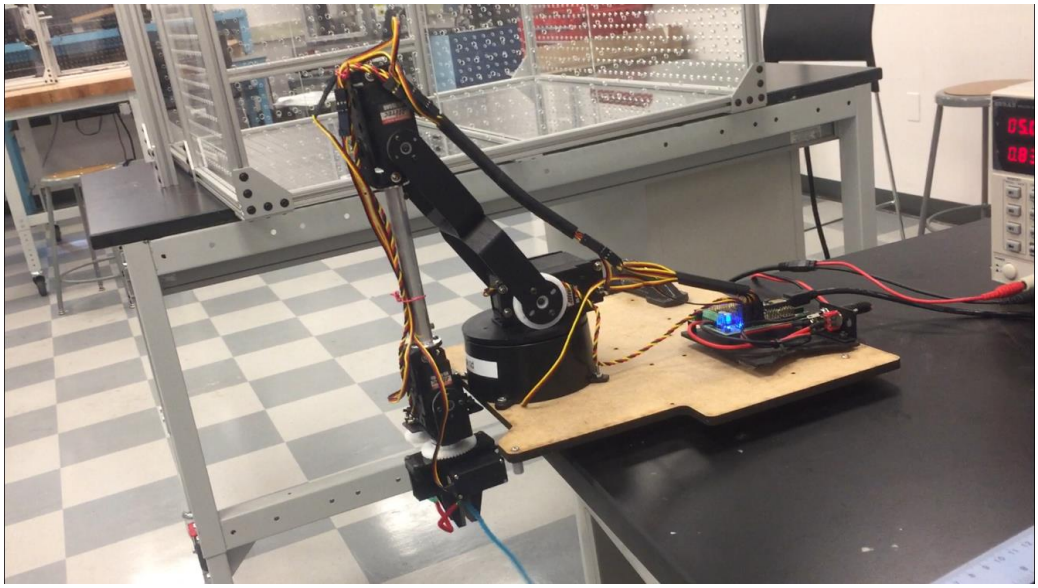

Figure 6-3 Conflict between end-effector and the front side of the table

(3) Constrains of the wire

The attached wire on the robot link 2 can be straighten out of its limit, so some simulated positions cannot be achieved by the physical robot.

This type of conflict is shown as Figure 6-4. There is a video (Video 4) showing the procedure of the conflict listed in Appendix 2.

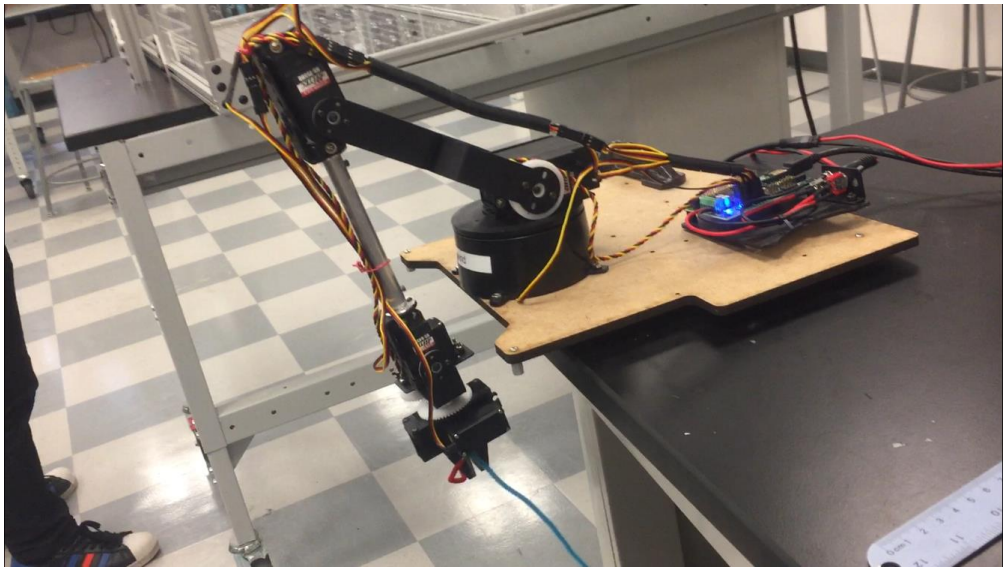

Figure 6-3 Constrain of the wire attached on link 2

There is a code simulating the conflict situations, *conflict.m*, listed in Appendix 1.

6.2 Method to determine the differences between simulated and physical workspace

As what is stated in 6.1, to determine the differences between the workspace of simulated and physical robot is to determine the workspace of the physical robot.

One method which is came up with is that after comprehensively and precisely measuring the characters of the robot and its working environment, modeling them with some CAD software (i.e. SolidWorks), and using the detect conflicts function of the software to simulate its physical workspace.

Therefore, I would need the geometry dimensions, material characters, and the basic information about the servos that its controller, to determine the differences between simulated and physical workspace.

Appendix 1 Code Overview

1.	*calculateFK_xzzhang.m*	compute forward kinematics
2.	*computeWorkspace_xzzhang.m*	compute simulated workspace
3.	*conflict.m*	simulate conflict situations
4.	*evaluation.m*	evaluate the homogenous matrices
5.	*lynxInitializeHardware.m*	predefined lynx function
6.	*lynxServo.m*	predefined lynx function
7.	*lynxServoSim.m*	predefined lynx function
8.	*lynxStart.m*	predefined lynx function
9.	*lynxVelocityPhysical.m*	predefined lynx function
10.	*plotLynx.m*	plot simulated configuration

Appendix 2 Video Overview

1.	https://youtu.be/7m2Y4vQomy0	conflict between links
2.	https://youtu.be/vYBgWekUVPc	conflict between links and table
3.	https://youtu.be/801Ah3JypX4	conflict between links and table
4.	https://youtu.be/Teol5a1c5mw	constrains of the wire